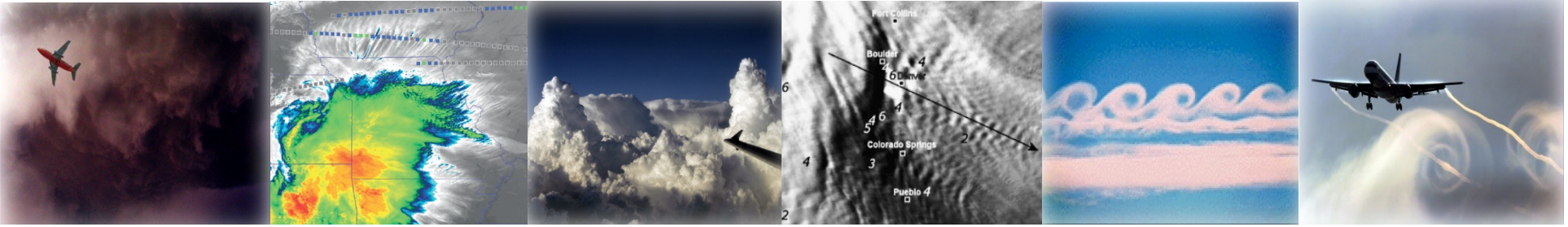

YONSEI UNIVERSITY

Atmospheric Turbulence in the Free Atmosphere Estimated using High Vertical-Resolution Radiosonde Data (HVRRD) and Thorpe Method

Hye-Yeong Chun and Han-Chang Ko
Department of Atmospheric Sciences, Yonsei University, Korea

Acknowledgement: *Marvin Geller, Bruce Ingleby and Robert Sharman*

The 3rd FISAPS Workshop, NCAR, USA, 2023.8.30-9.1

Outline

- Introduction
- Thorpe's method
- Characteristics and potential sources of the estimated turbulence in the troposphere and stratosphere in USA (Ko and Chun 2022, AR)
- Global distribution of atmospheric turbulence using the operational radiosonde data of ECMWF (Ko, Chun, Geller, and Ingleby, 2023, in prep.)
- Some issues and on-going research

Introduction

- **Observational turbulence studies in the free atmosphere** have mainly been conducted using **radar, aircraft, and rocket observations** (Lübken, 1992; Nastrom and Eaton, 1997; Cho et al., 2003; Singh et al., 2008; Sharman et al., 2014), although **geographical coverage of those instruments is limited**.
- **High vertical resolution radiosonde data (HVRRD)** with **1-second resolution (~5 m)** have been archived (Ingleby et al. 2016) at weather forecasting centers, and they are widely used not only for **numerical weather prediction** but for various researches such as **gravity waves** (Wang and Geller 2003), **turbulence** (Ko et al. 2019, 2022), and **boundary-layer depth** (Yan et al. 2021**).**
- Estimation of atmospheric turbulence in the free atmosphere based on the **Thorpe method (1977) using HVRRD** has been conducted over various regions (Clayson and Kantha 2008; Muhsin et al. 2016; Zhang et al. 2019; Geller et al. 2021; Ko and Chun 2019, 2022), and it is compared with that estimated from **radar** (Kohoma et al. 2019) and **LITOS** (Schneider et al. 2015) observations and **direct numerical simulation** results (Fritts et al. 2016).
- Recently, **comparison of EDR** (1/3 power of the eddy dissipation rate) observed **in situ from aircrafts** with that estimated using **Thorpe method and HVRRD** along the main flight routes of **USA for 6 years (2012-2017)** has been made (Ko et al. 2023, JGR in minor revision), and **similarities and differences** are investigated.

Method (Thorpe's Method)

"Resorting" (Thorpe 1977)

Red: observed potential temperature
Blue: resorted potential temperature

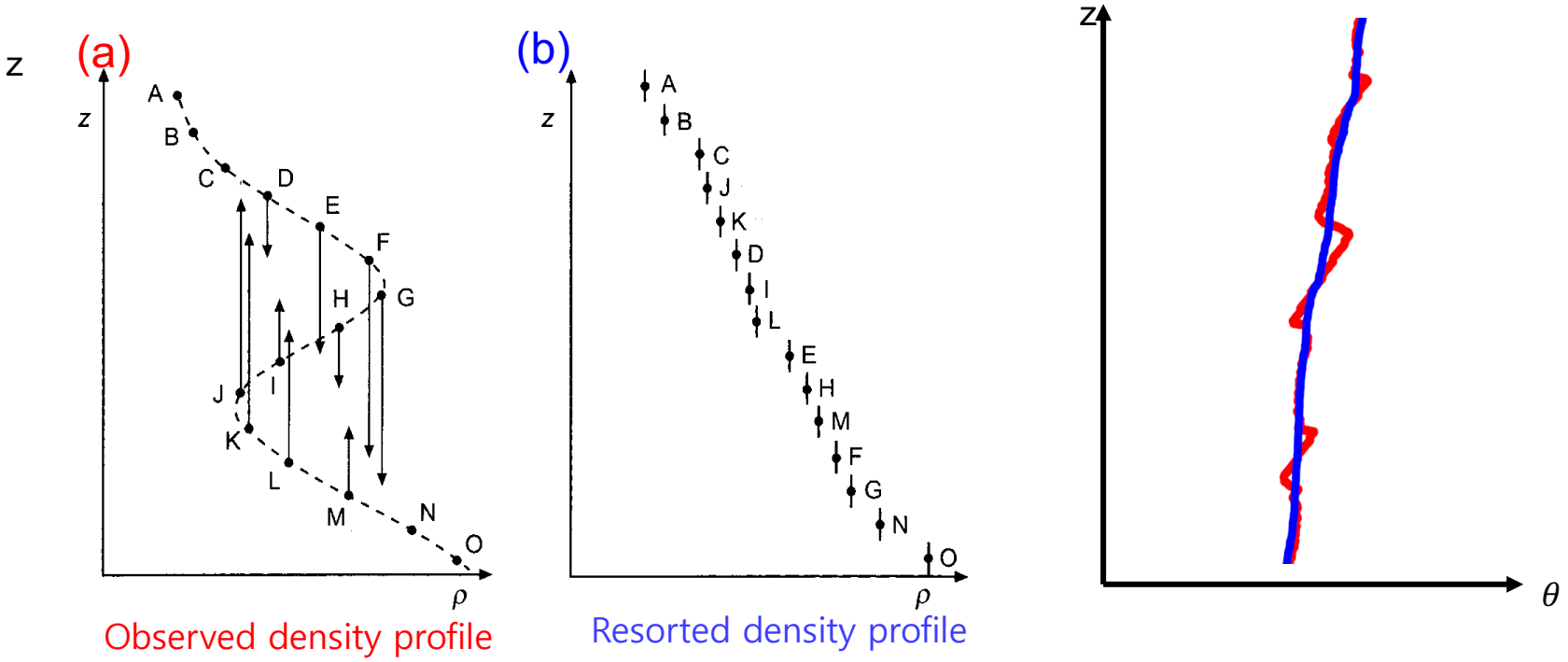

- The observed profile of density (a) is vertically displaced by turbulent motion, from (b) a stable basic-state profile without time for significant molecular diffusion to occur.
- In the atmosphere, potential temperature can be used (Clayson and Kantha, 2008).
- This method is applied to the free atmosphere

Estimation of eddy dissipation rate using Thorpe's method

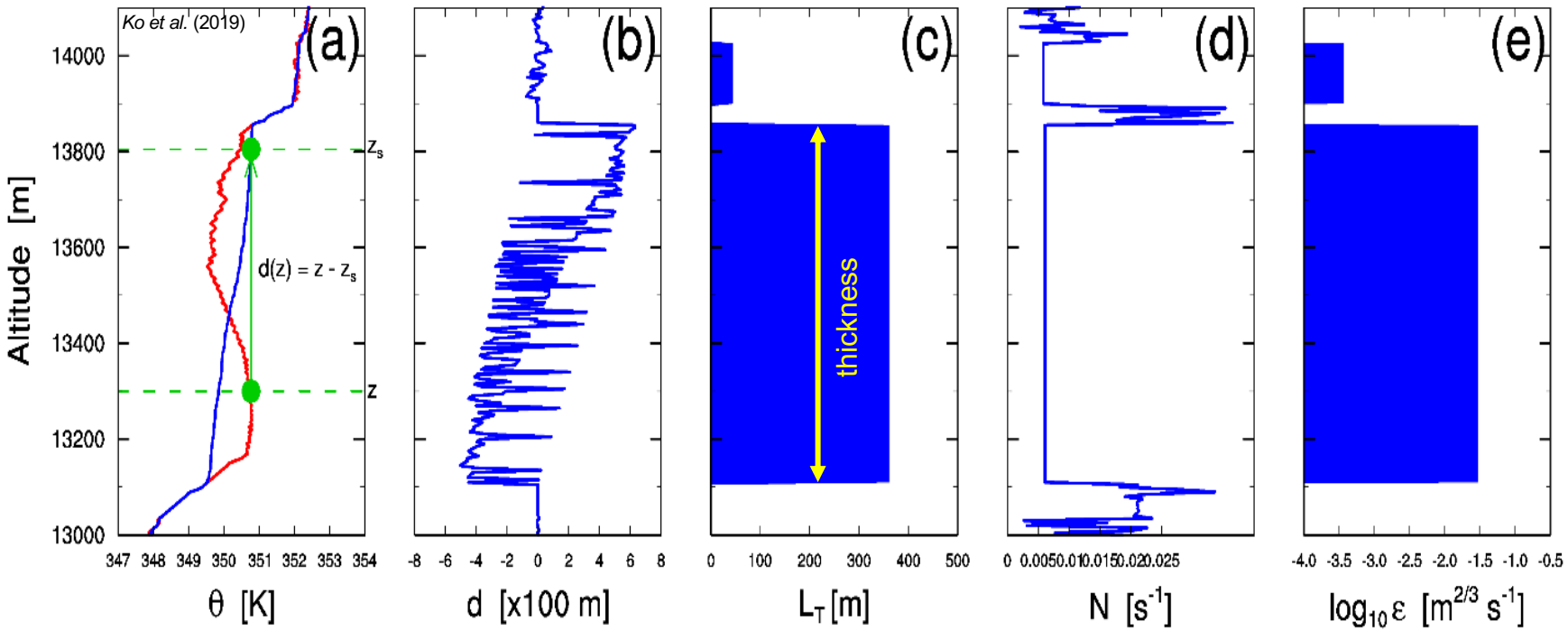

red: observed θ
blue: stably sorted θ

- $d = z - z_s$ is defined as Thorpe displacement, and whose root-mean-square (rms) value in detected turbulent layer is Thorpe scale (L_T).
- Thorpe scale is correlated with the Ozmidov scale [$L_o \equiv (\varepsilon/N^3)^{1/2}$].

Using $L_o = cL_T$,

$$\varepsilon = C_K {L_T}^2 N^3 \text{ where } C_K = c^2.$$

C_K=0.3: Clayson and Kantha (2008)
C_K=1.0: Kantha and Hocking (2011), Li et al. (2016), Ko et al. (2019)

- Instrumental noise (Wilson et al. 2010; 2011) and moist-saturation effects (Wilson et al. 2013) are considered

Characteristics and potential sources of the estimated turbulence in the troposphere and stratosphere in USA

Ko and Chun (2022, Atmospheric Research)

Data

	Operational high vertical-resolution radiosonde data (HVRRD)
No. of stations	68
Resolution	1 s (~5 m vertically)
Observations	P, T, Rh, U, V, z
Launch frequency	twice a day (00 and 12 UTC)
Data period	Jan. 2012-Dec. 2017 (6 years)

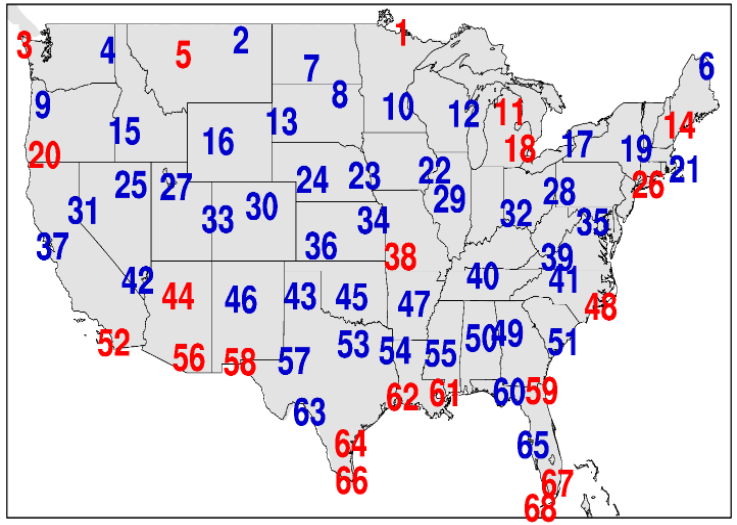

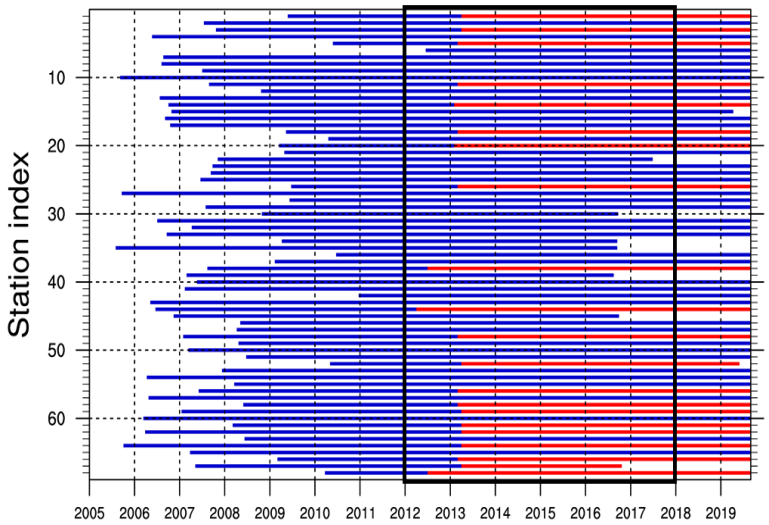

blue: Lockheed Martin LMS-MkIIa: **212,023** profiles
red: Väisälä RS92-NGP: **72,378** profiles

As the transition of radiosonde instruments can significantly affect the turbulence estimation (**Geller et al. 2021, MWR**), we used the data exclusively from the Lockheed Martin LMS-MkIIa.

Monthly occurrence frequency of unstable layers of thickness 10-400m (z=15-25 km)

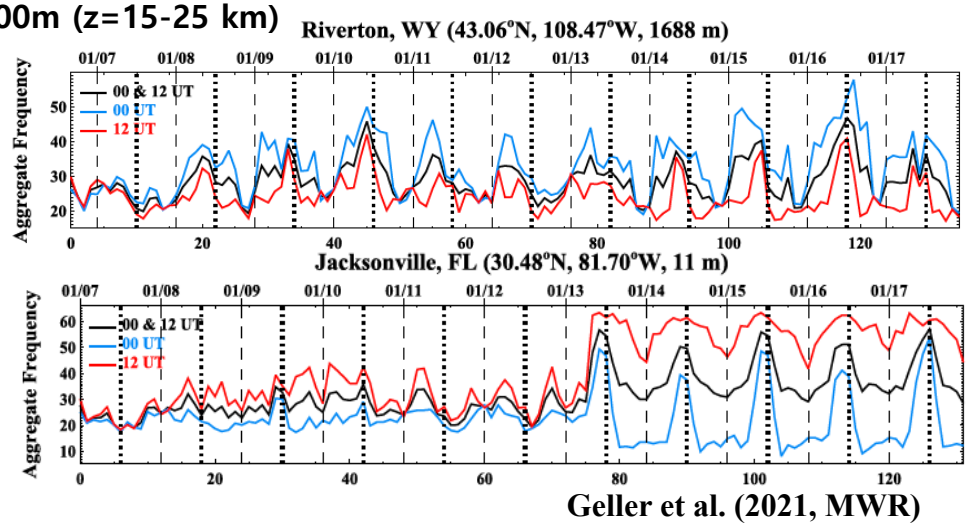

Geller et al. (2021, MWR)

Characteristics of turbulence retrieved from HVRRD

Troposphere(TR): 3km-tropopause

Stratosphere(ST): tropopause-30km

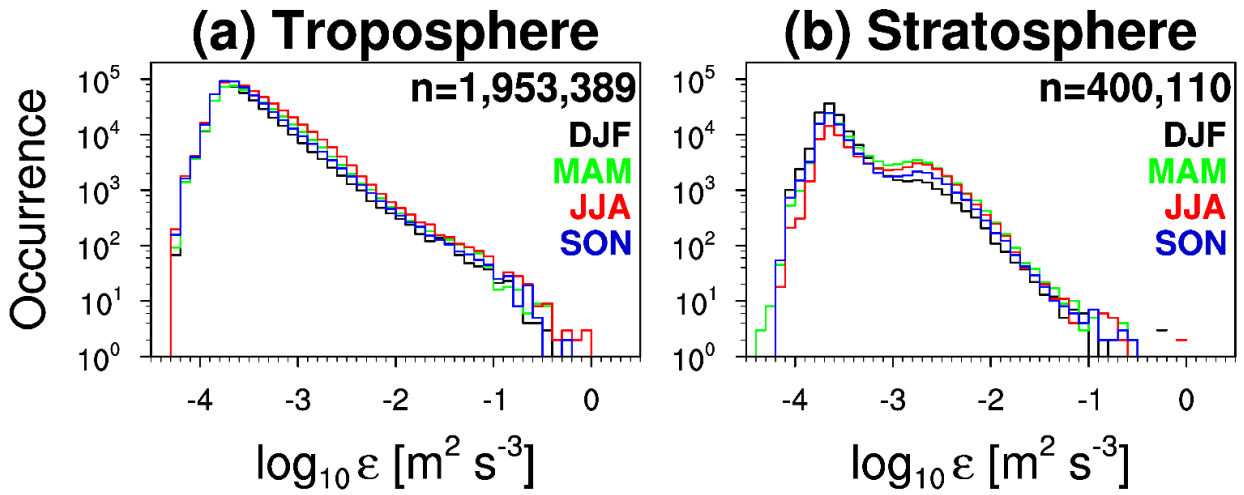

- More strong turbulence ($\log_{10}\varepsilon$>-3 m^2 s^{-3}) in TR than in ST.
- Largest in JJA in TR, less evident in ST

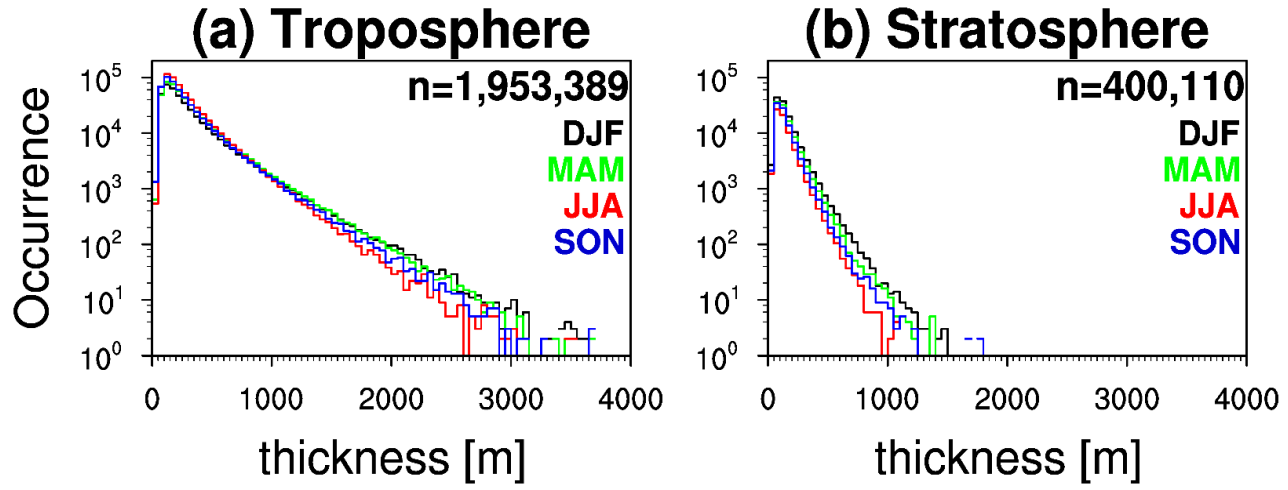

- Mean(median) thickness is 278(205)m in TR and 140(115) in ST.
- Largest in JJA for small thickness (<1000m) and in DJF for large thickness (>1000m) in TR, and largest in DJF in ST

Horizontal distributions of layer-mean thickness of turbulence layer (THTL)

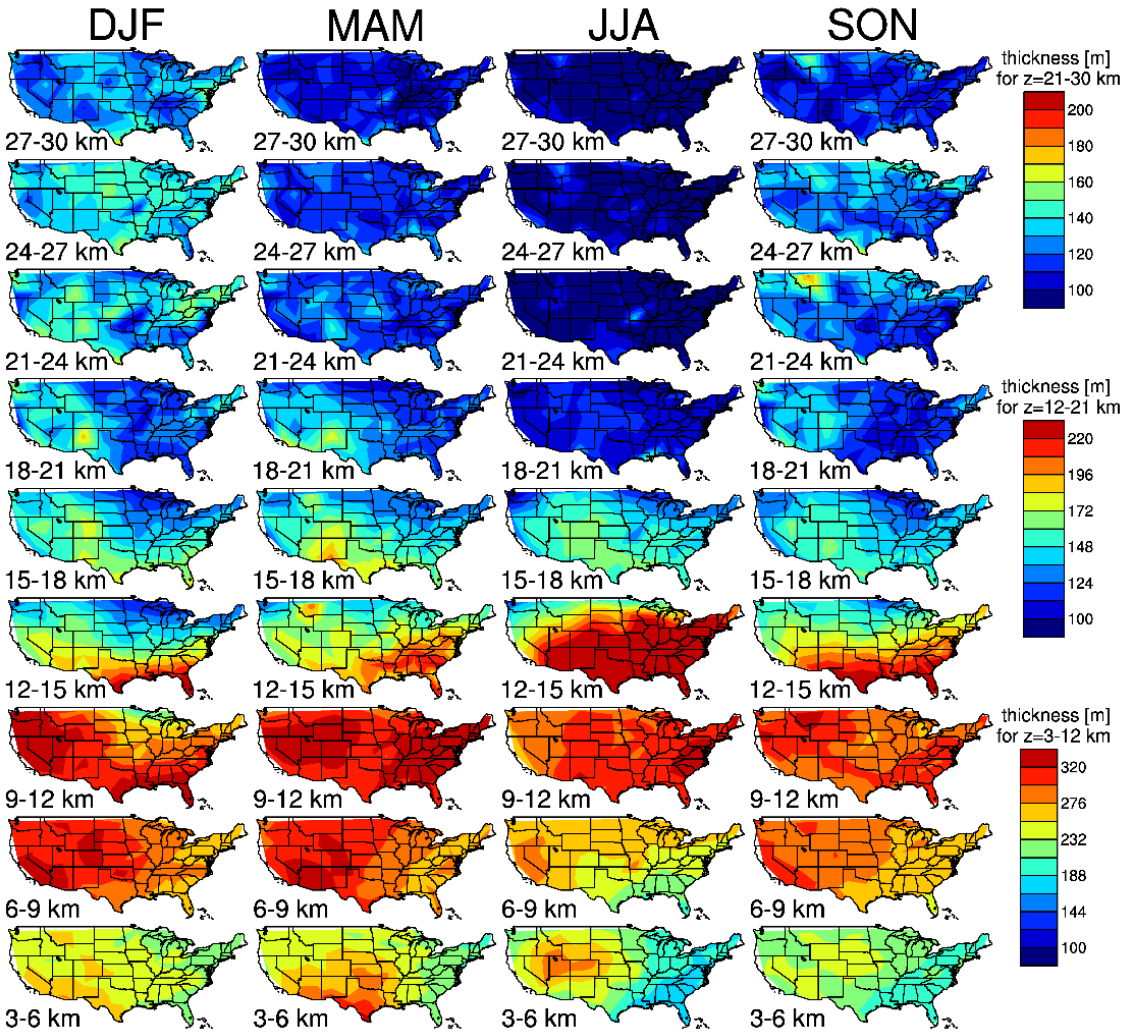

- Layer-mean THTL increases as altitude increases below z=12 km but decreases above z=12 km.
- Below z=12 km, layer-mean THTL is large in DJF and MAM
- Above z=15 km, layer-mean THTL is largest in DJF and smallest in JJA.
- Regionally, at z=3–21 km, layer-mean THTL shows large values in western mountainous region and the southeastern region.

layer-mean THTL $= \frac{\sum \text{THTL}}{n}$, where n is the occurrence number of non-zero THTL in each altitude bin

Horizontal distributions of layer-mean $\log_{10}\varepsilon$

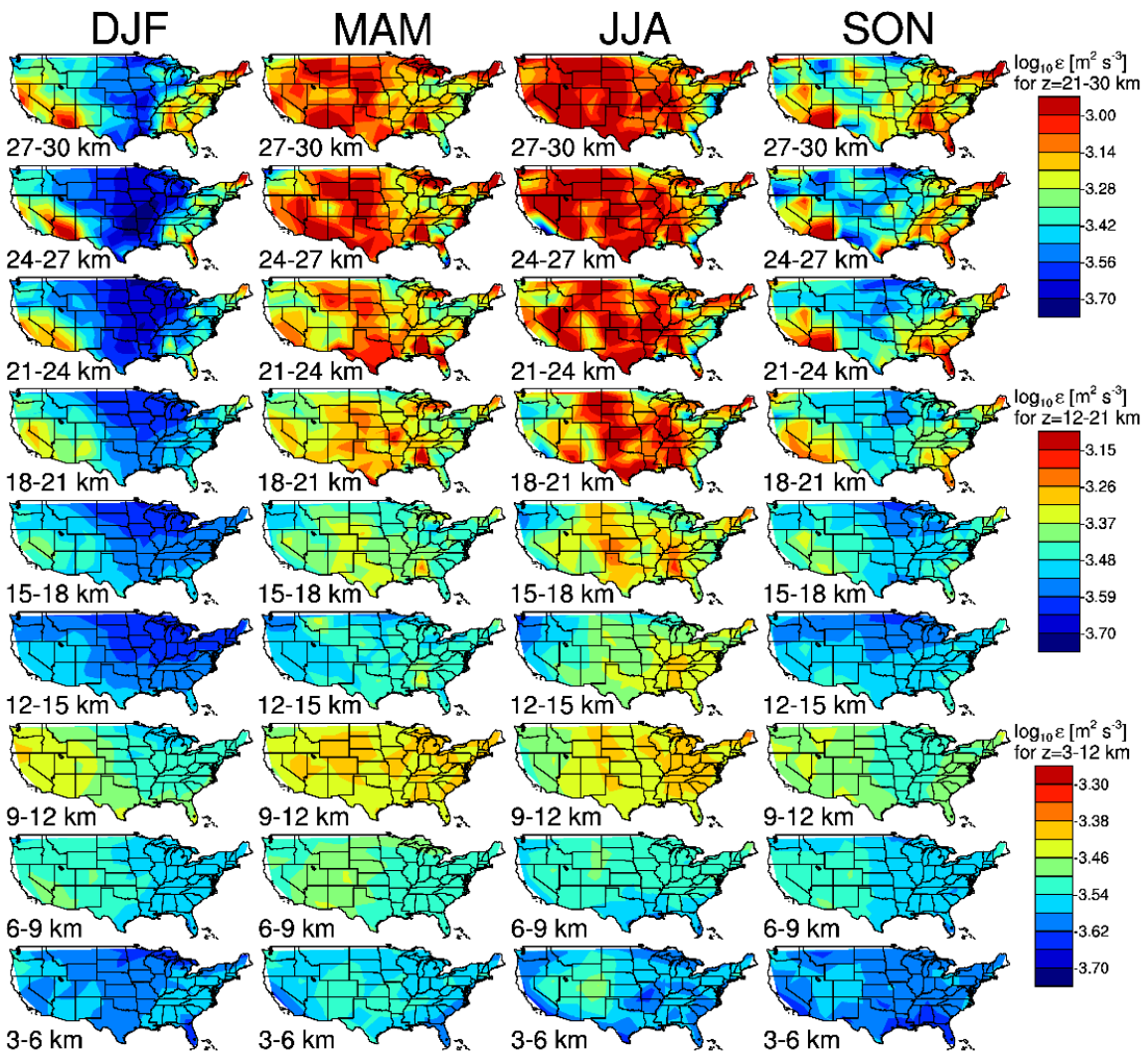

- The seasonal-altitudinal variations of $\log_{10}\varepsilon$ are opposite to those of layer-mean THTL, with large values at high altitudes and in JJA.
- However, the regional pattern is generally consistent with that of the layer-mean THTL
- **Large layer-mean $\log_{10}\varepsilon$ in the high altitudes stems from the smaller number of turbulence cases in the stratosphere than in the troposphere.**

layer-mean $\log_{10}\varepsilon = \frac{\Sigma \log_{10}\varepsilon}{n}$, where n is the occurrence number of non-zero $\log_{10}\varepsilon$ in each altitude bin

Layer-mean effective eddy dissipation rate (EE)

- A simple layer-mean $\log_{10}\varepsilon$ does not properly represent characteristics of turbulence in each layer.
- To better represent the layer-mean turbulence accounting **vertical portion of the turbulence occupation in each bin**, a new quantity, **layer-mean effective ε (EE)**, is proposed.

Layer-mean effective ε (EE):

$$\frac{\sum \varepsilon \times \mathrm{THTL}}{Z} \quad [\mathrm{m^2\ s^{-3}}],$$

where Z is the layer depth (3 km in this study) of each altitude bin.

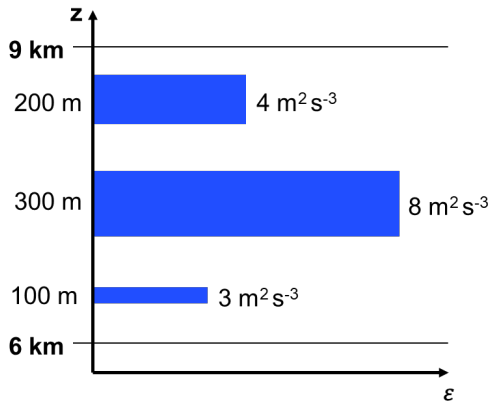

Horizontal distributions of EE

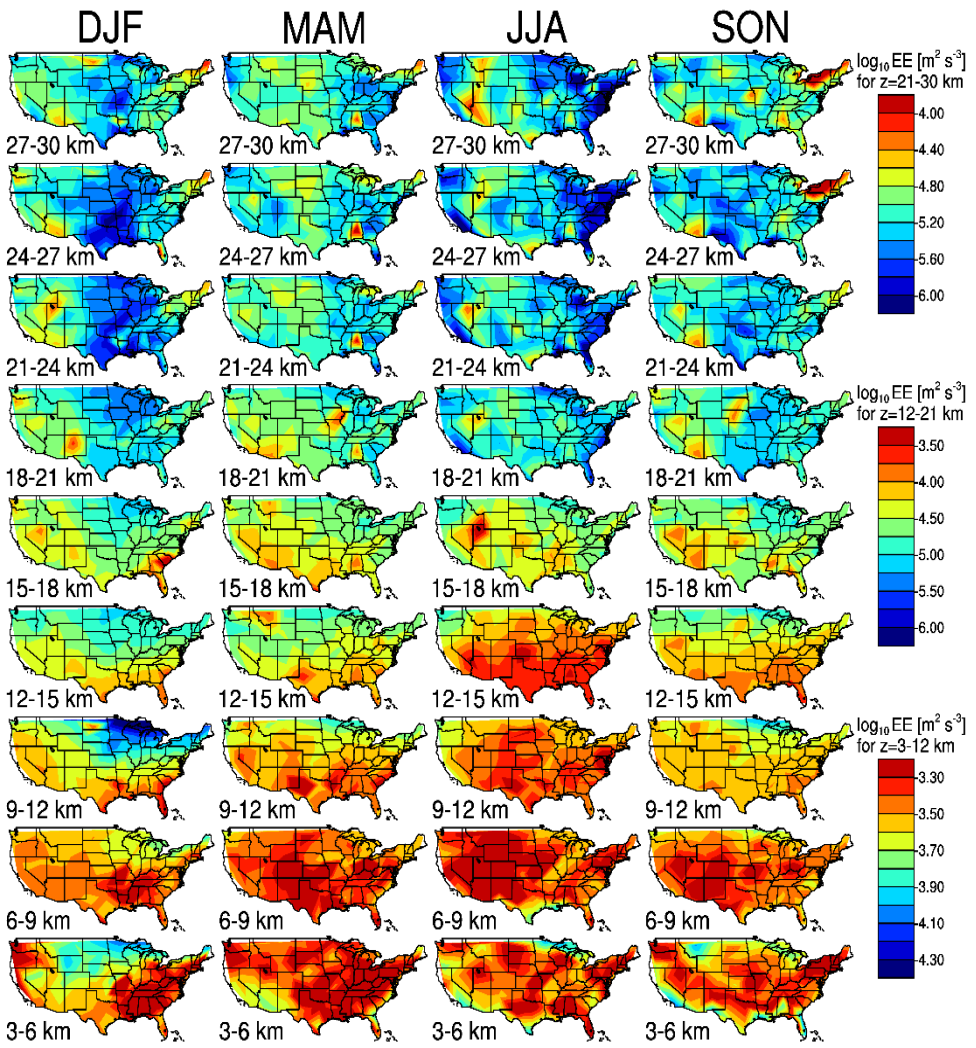

EE: $\frac{(3\times100 + 8\times300 + 4\times200 + 0\times2400)\ [\mathrm{m^2\ s^{-3}}][\mathrm{m}]}{3000\ [\mathrm{m}]}$

Potential Sources of HVRRD-estimated Turbulence

Turbulence indices are calculated using ERA5 reanalysis

	ERA5 Reanalysis
Horizontal resolution	0.25 x 0.25 [deg]
No. of vertical levels	37 (top: 1 hPa)
Time period	1 hourly
Data period	Jan. 2012-Dec. 2017 (6 years)

Vertical grid spacing of ERA5 Reanalysis

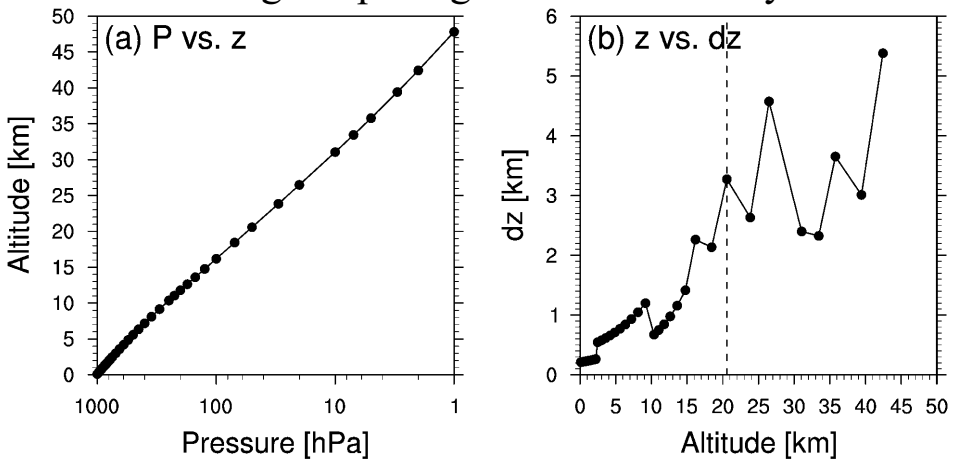

Above ~21 km, vertical grid spacings are ~3 km
→ Results below z=21 km are shown

- Squared Brunt-Vaisala frequency $N^2 = \frac{\theta}{g}\frac{\partial \theta}{\partial z}$
- Vertical wind shear (VWS) $= \sqrt{\left(\frac{\partial u}{\partial z}\right)^2 + \left(\frac{\partial v}{\partial z}\right)^2}$
- Orographic gravity wave drag (OGWD) $= -\frac{1}{\rho}\frac{\partial \tau}{\partial z}$ Palmer et al. (1986), Chun et al. (1996)
- Convective precipitation

Horizontal Distributions of Turbulence Indices

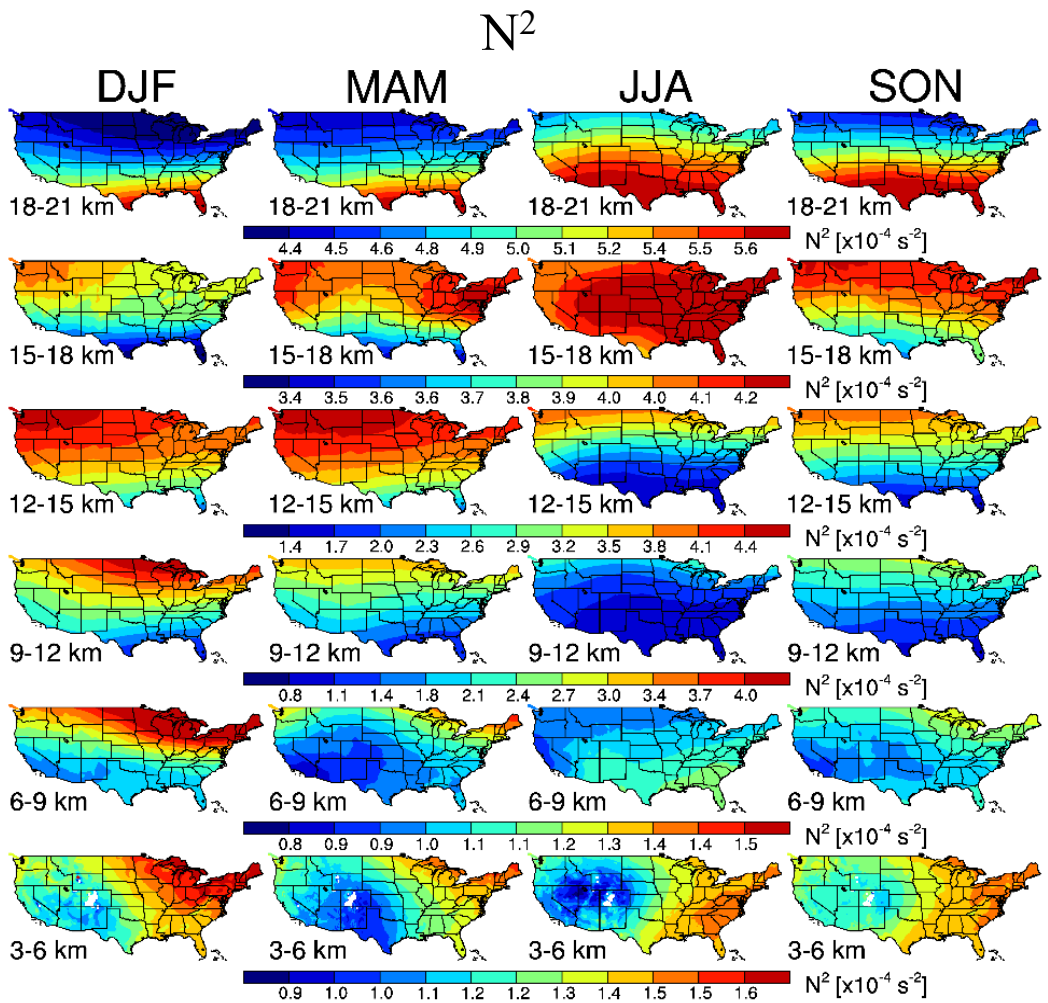

- At z = 3–6 km, weak in western mountain regions, especially in JJA.
- At z = 6–15 km, latitudinal variations are dominant and weak in JJA.
- At z = 18–21 km, strong at low latitudes because the latitudinal temperature structure is opposite to that below in the mid-latitudes (Holton, 2004).

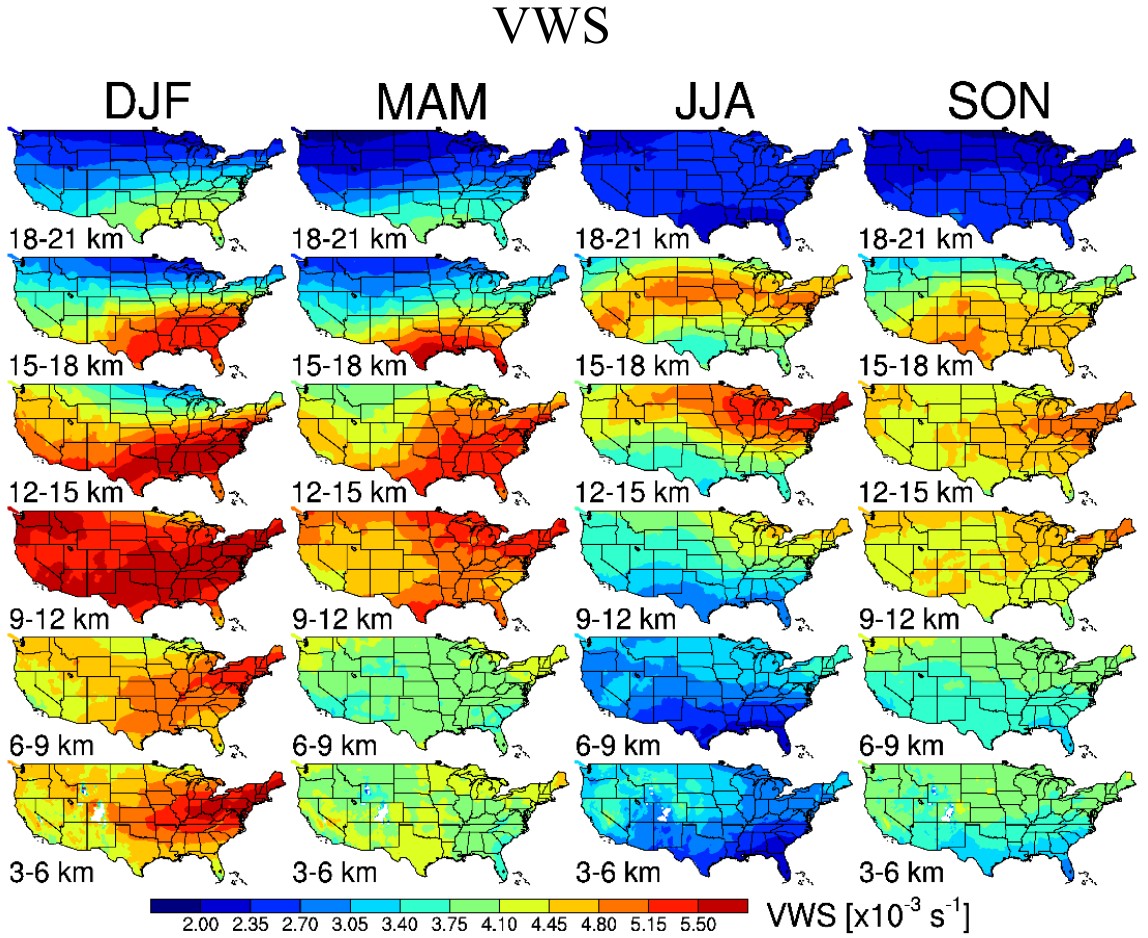

- Large values appear in Eastern USA in most altitudes and seasons, with largest in DJF at z=9–12 km, which can be attributed to the strong jet stream in the Eastern United States (Koch et al., 2006).
- At z = 18–21 km, VWS is much smaller than that below, due to small vertical variation of the large-scale wind in the mid-latitude stratosphere (Holton, 2004).

Horizontal Distributions of Turbulence Indices

OGWD

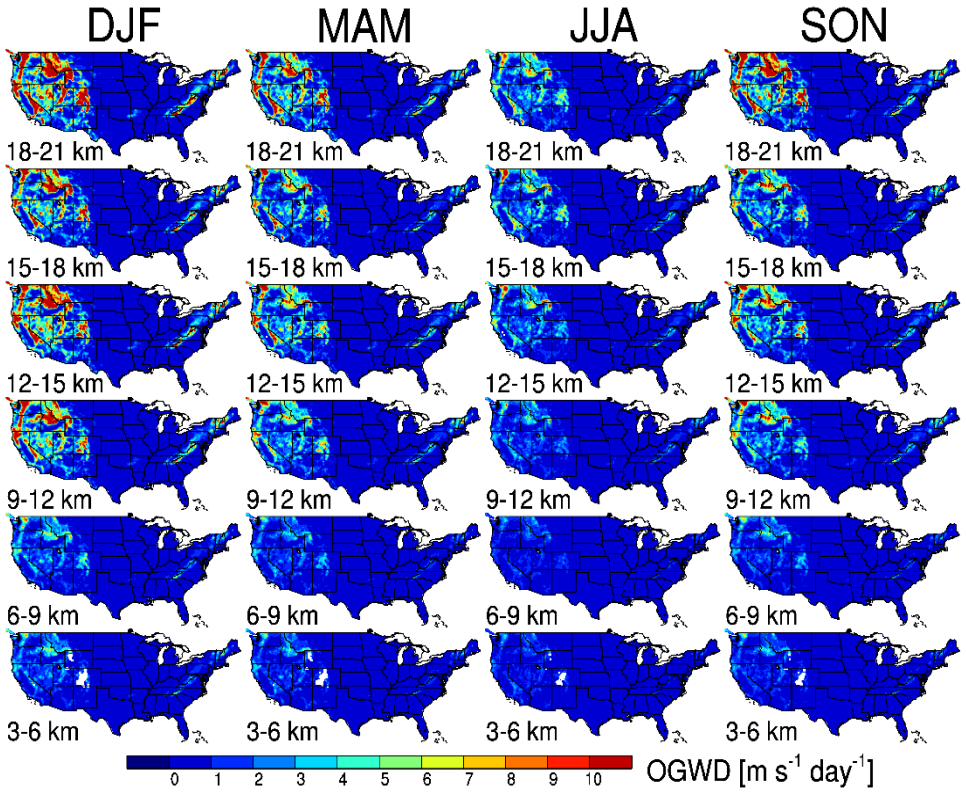

- Stronger OGWD appears in western mountain regions with secondary peaks near eastern mountain regions.
- OGWD shows clear seasonal variations, largest in DJF and smallest in JJA, and intensity of OGWD increases with altitude, as expected.

Convective precipitation

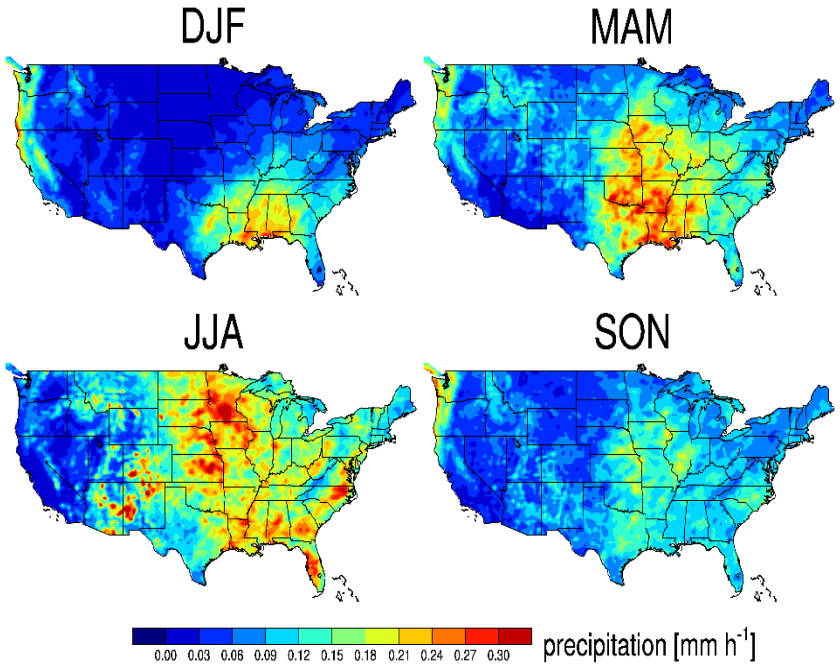

- Convective precipitation is largest in JJA throughout the Eastern United States.
- Strong convective precipitation in the west coast of the United States in DJF, MAM, and SON.

Correlation between monthly-mean of EE and turbulence indices

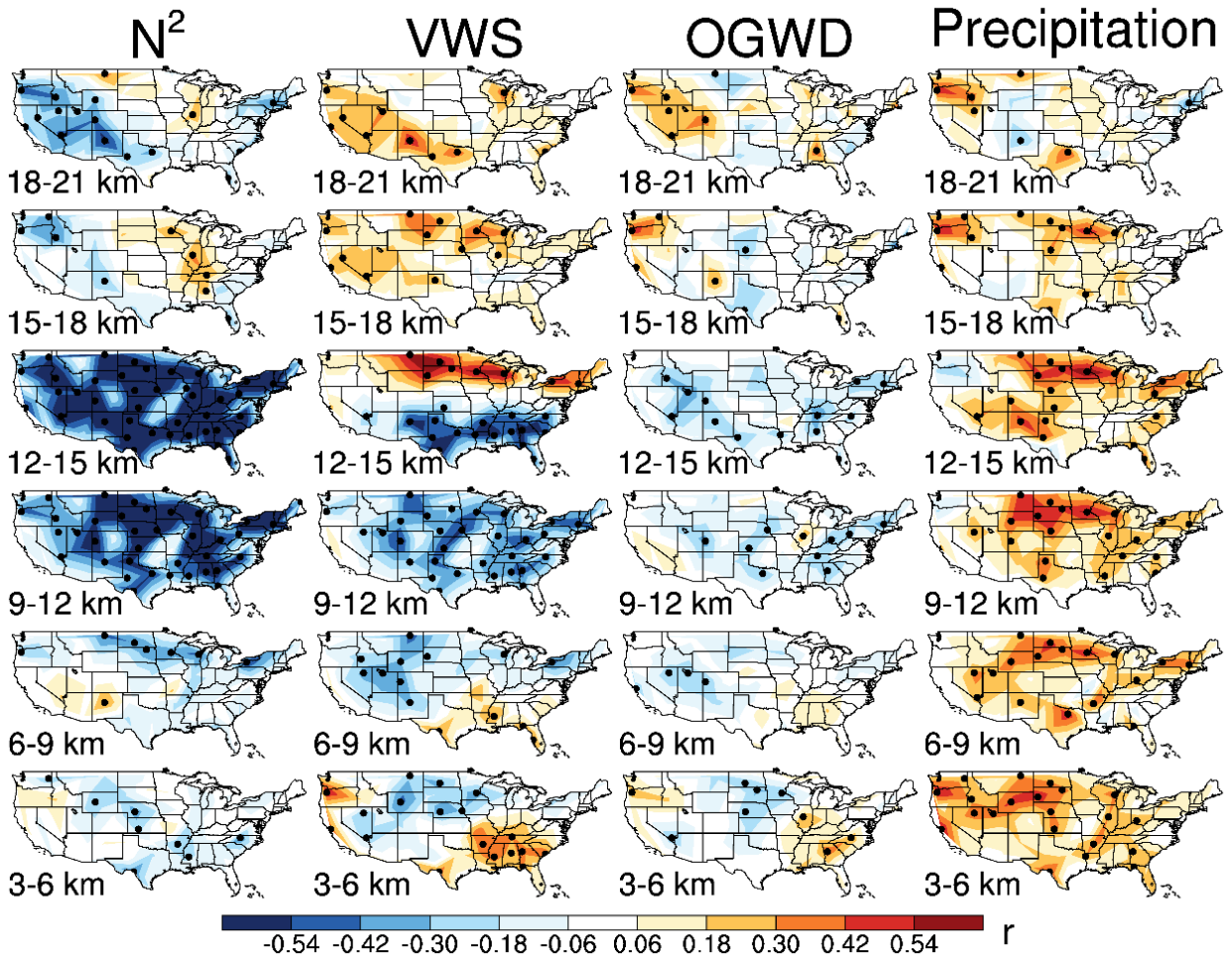

dot: the stations for which the r is significant at the 95% confidence level.

- In most regions, EE and N^2 (Precipitation) is negatively (positively) correlated.
- VWS and OGWD are correlated with EE under specific conditions and in certain locations: VWS is positively correlated under strong stability and OGWD is positively correlated in western mountain regions at z = 15–21 km.

Global Distributions of Atmospheric Turbulence Estimated Using Operational High Vertical-Resolution Radiosonde Data

Ko, Chun, Geller, and Ingleby (2023, in prep.)

Locations of radiosonde stations providing 1-s or 2-s data of ECMWF

Oct. 2014 – Dec. 2021 (87 months)

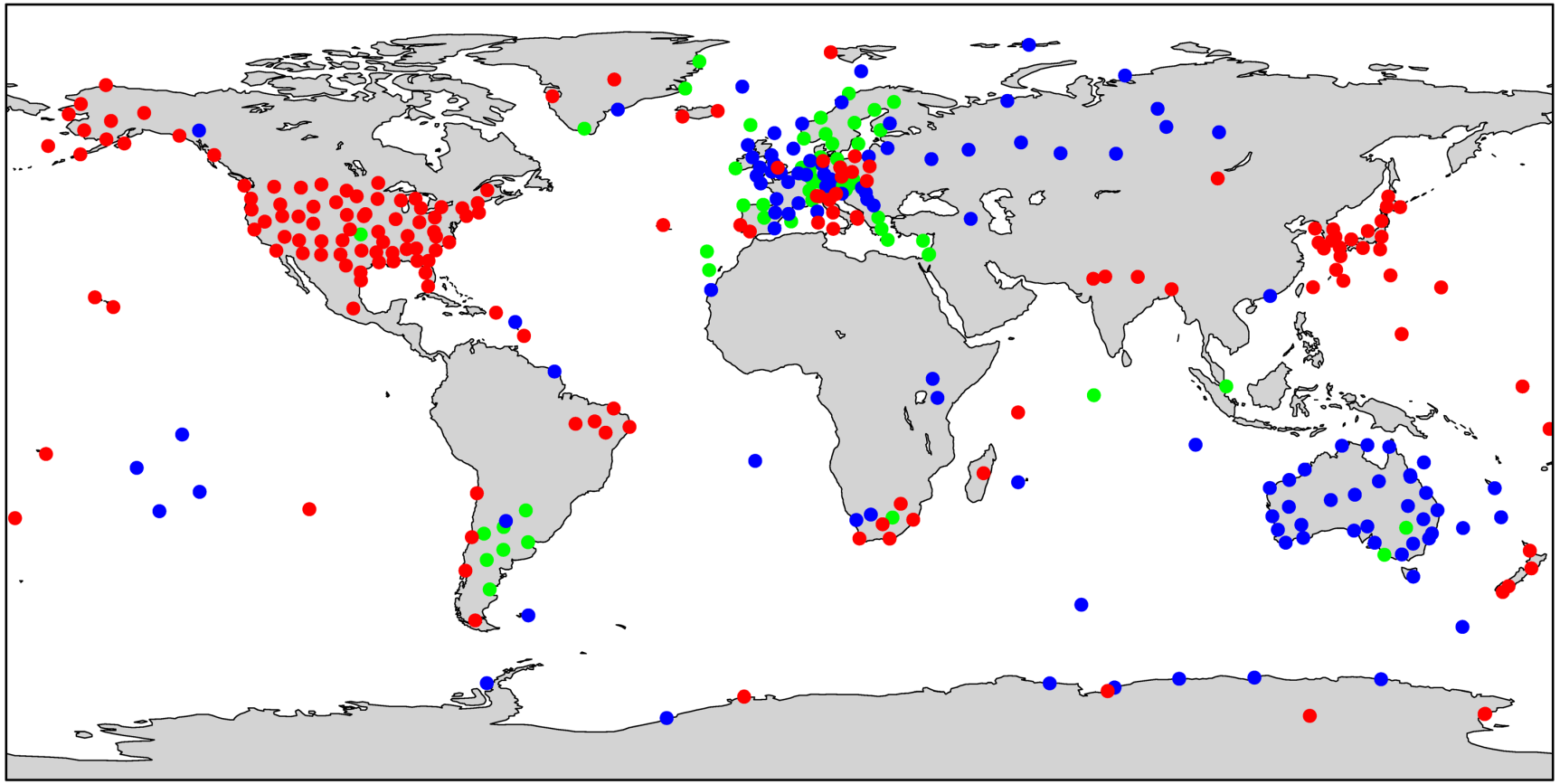

only 1-s (164) only 2-s (111) 1-s and 2-s (58) total: 333

- ✓ **Only 1-s**: During given period, stations that provide only 1-s resolution radiosonde data
- ✓ **Only 2-s**: During given period, stations that provide only 2-s resolution radiosonde data
- ✓ **1-s and 2-s**: During given period, stations that provide both 1-s and 2-s resolution radiosonde data

Monthly number of radiosonde stations that provide 1-s or 2-s res. data

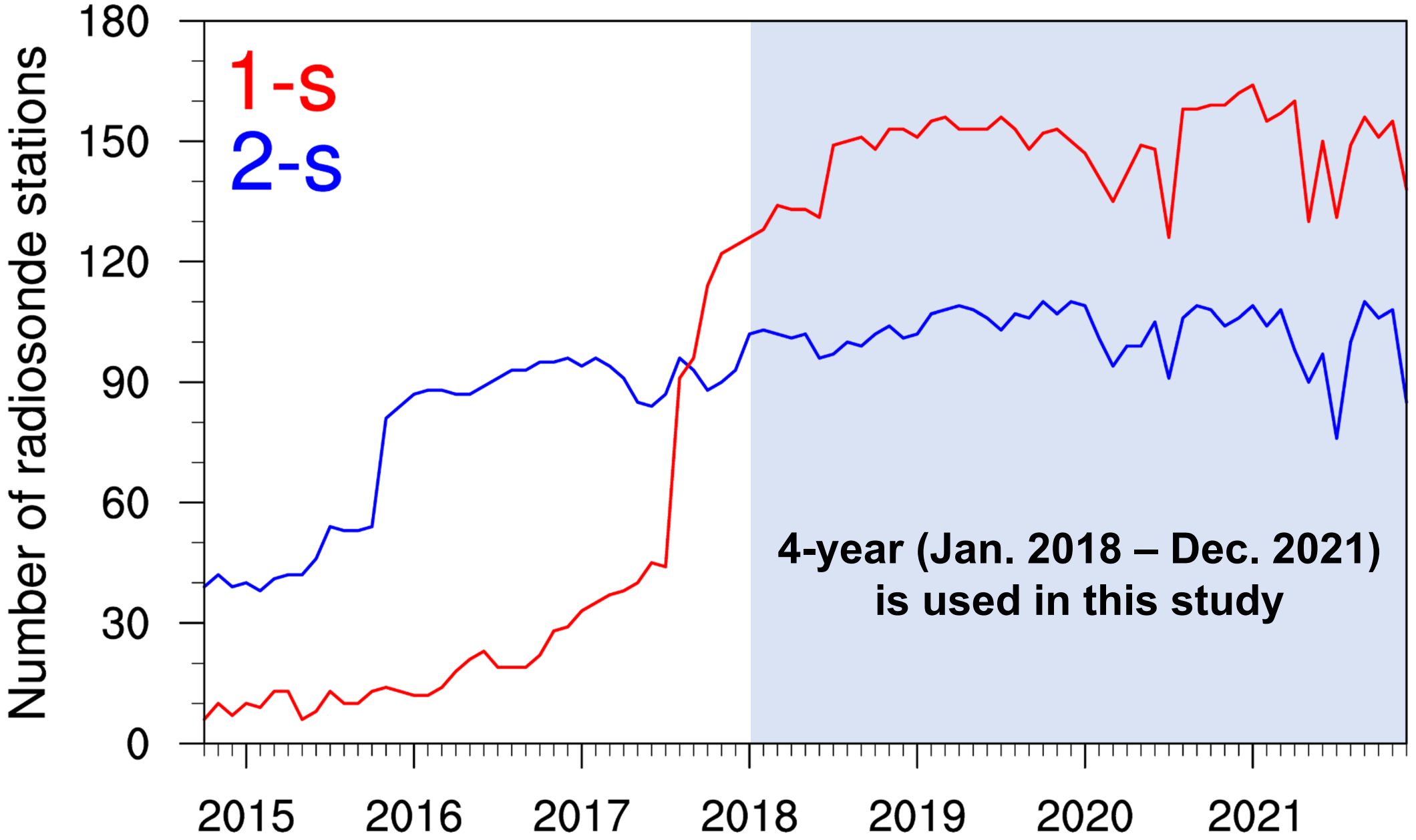

Locations of radiosonde stations that provide 1-s or 2-s res. data

Jan. 2018 – Dec. 2021 (4 years)

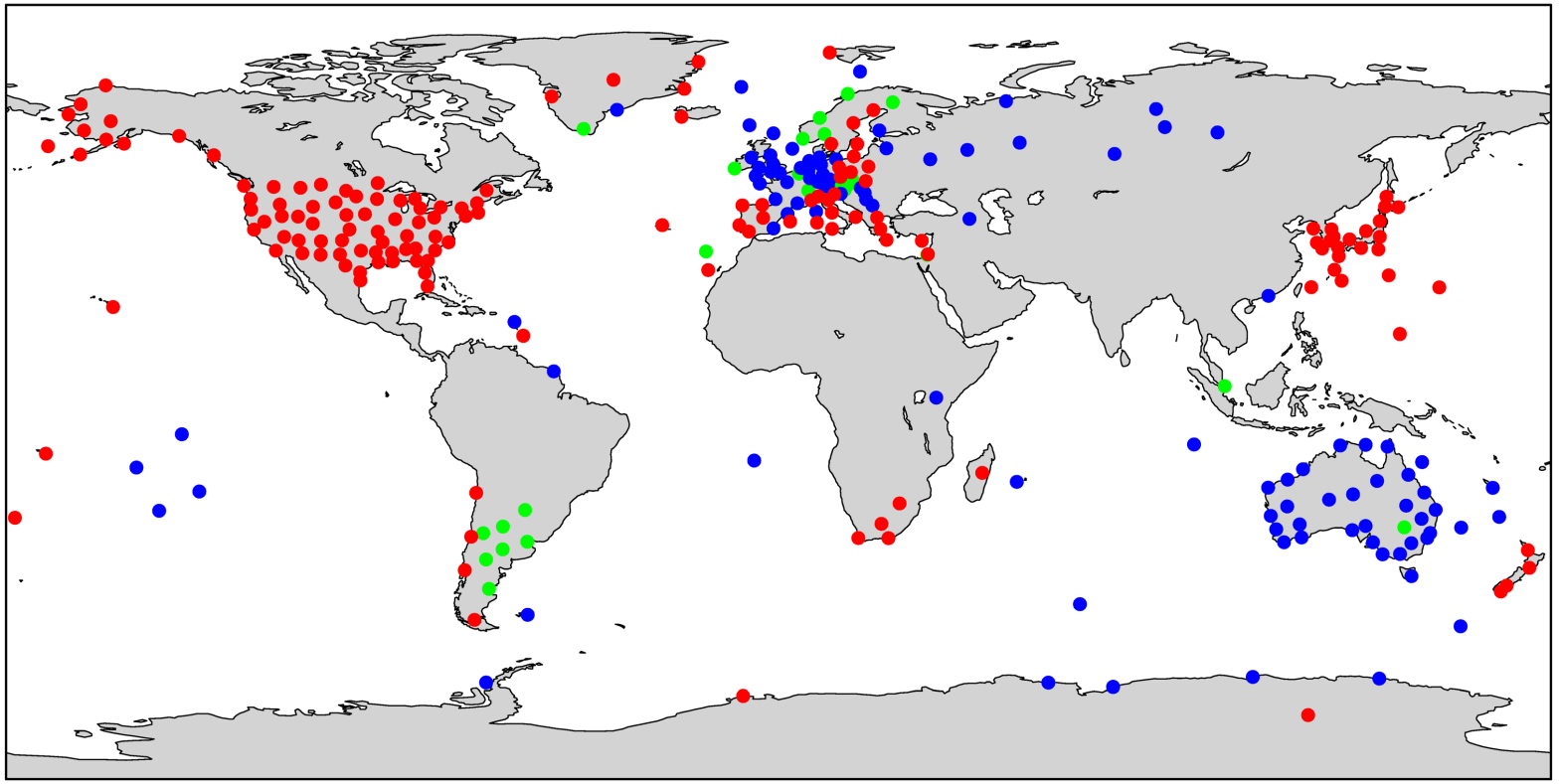

only 1-s (151) only 2-s (101) 1-s and 2-s (27) total: 279

No. of stations	NH	SH	sum
only 1-s	134	17	151
only 2-s	52	49	101
1-s and 2-s	19	8	27
sum	205	74	279

1-s and 2-s data are vertically interpolated into 5 m and 10 m, respectively, using cubic-spline interpolation.

Occurrence numbers of $\log_{10}\varepsilon$ and turbulence thickness layer (THTL)

Jan. 2018 – Dec. 2021 (4 years)

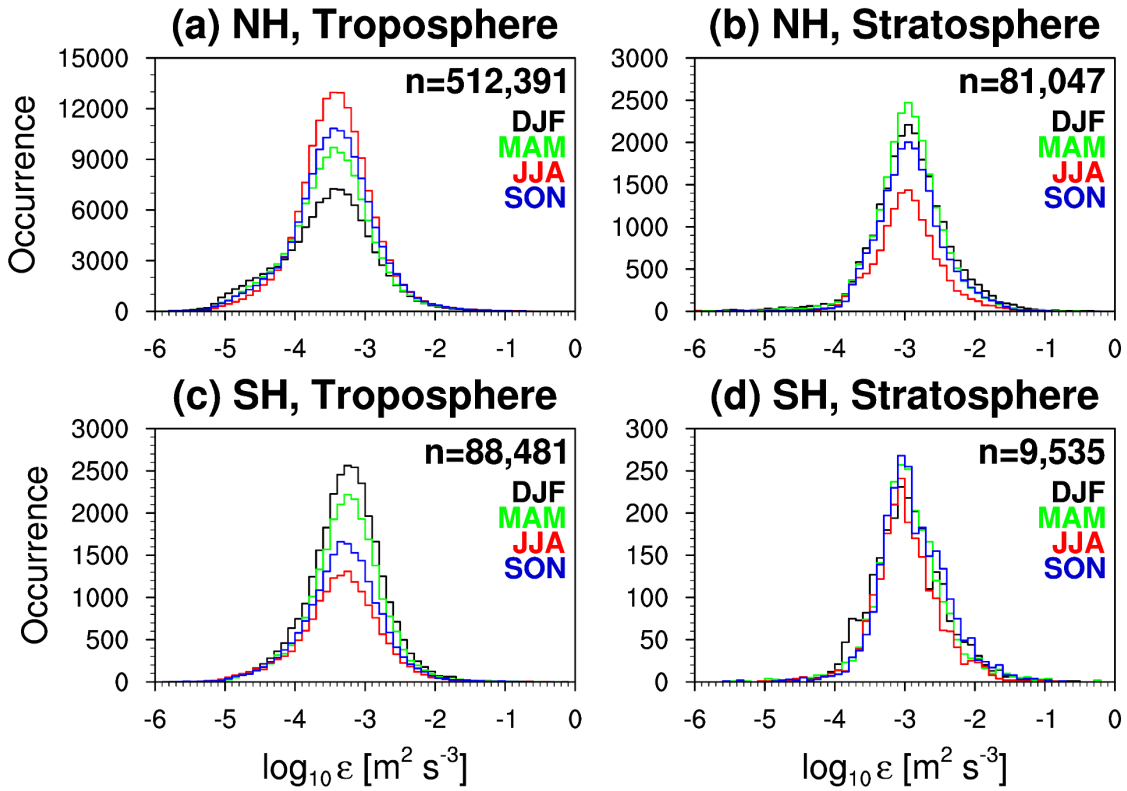

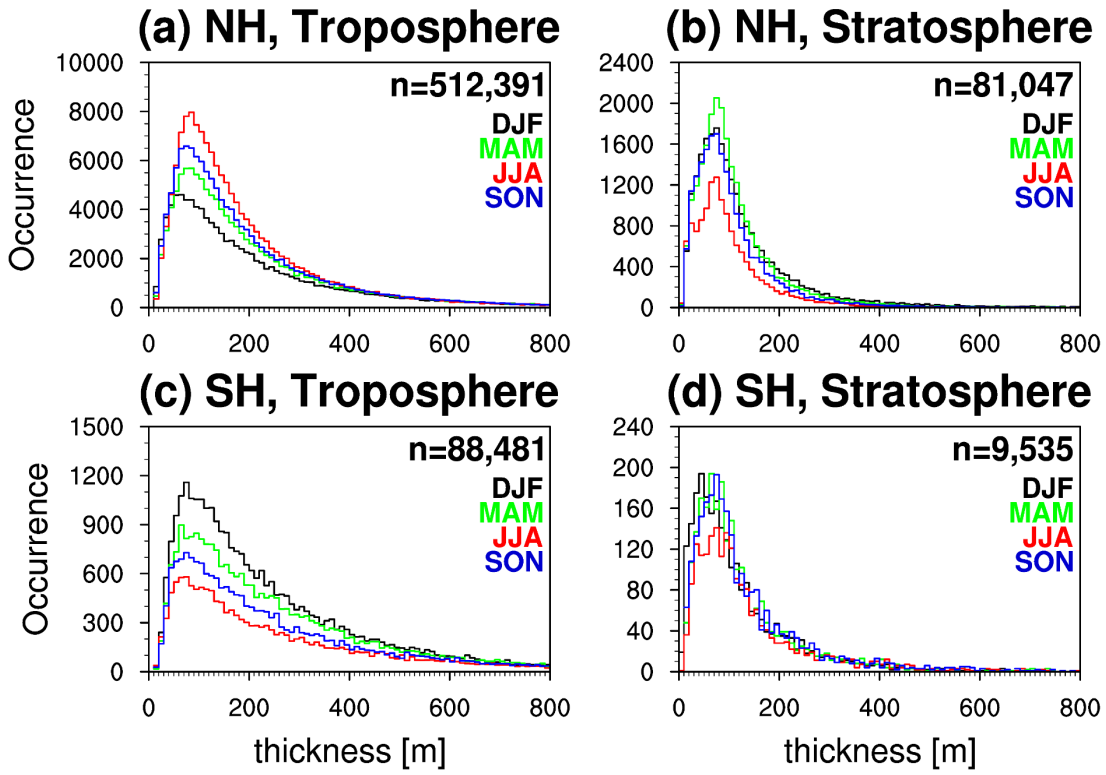

- Strong seasonal variations: maximum in summer and minimum in winter in the troposphere, while spring maximum in the stratosphere.

- More cases of thick THTL in the troposphere than in the stratosphere, with strong seasonal variations in the troposphere.

- ✓ **Troposphere**: 3 km above the station height – tropopause*
- ✓ **Stratosphere**: tropopause – 30 km
- ✓ *tropopause is calculated by the definition of WMO (1957)
- ✓ "n" denotes the total occurrence number of turbulence in each altitude range

Horizontal distribution of layer-mean effective ε (EE)

2018 – 2021 (4 years)

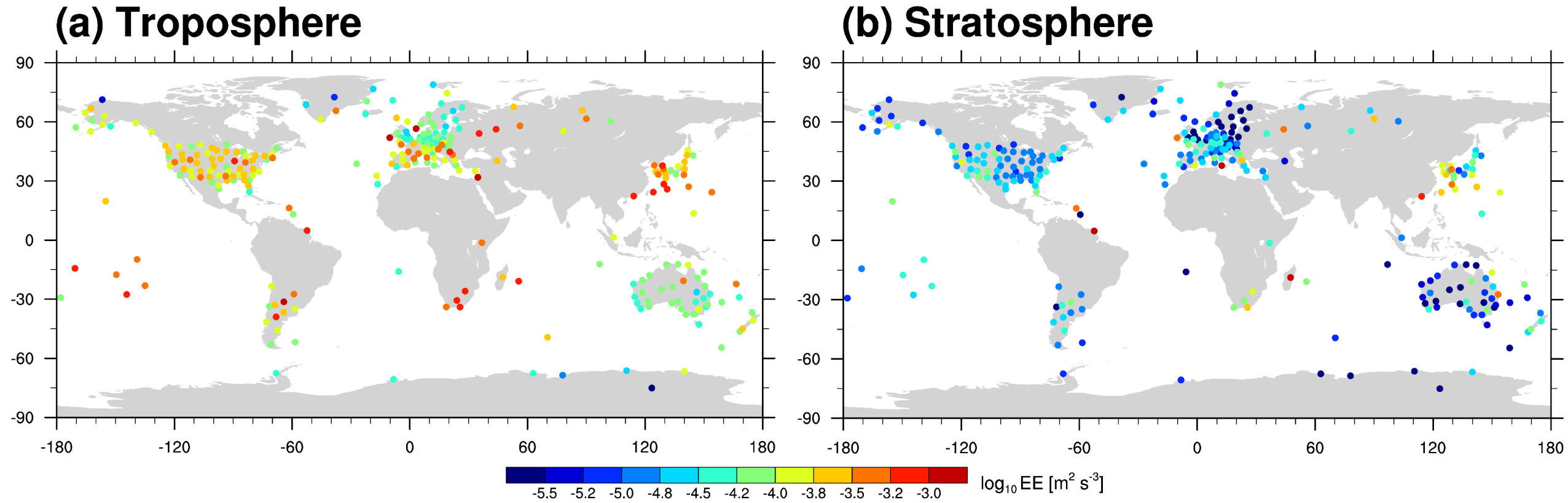

- Globally, EE is much larger in the troposphere than in the stratosphere.
- In the troposphere, local peaks appear in the East Asia, Europe, South America, South Africa, and Pacific islands.
- In the stratosphere, local peaks appear in East Asia, South Africa, and South America

Regional analysis

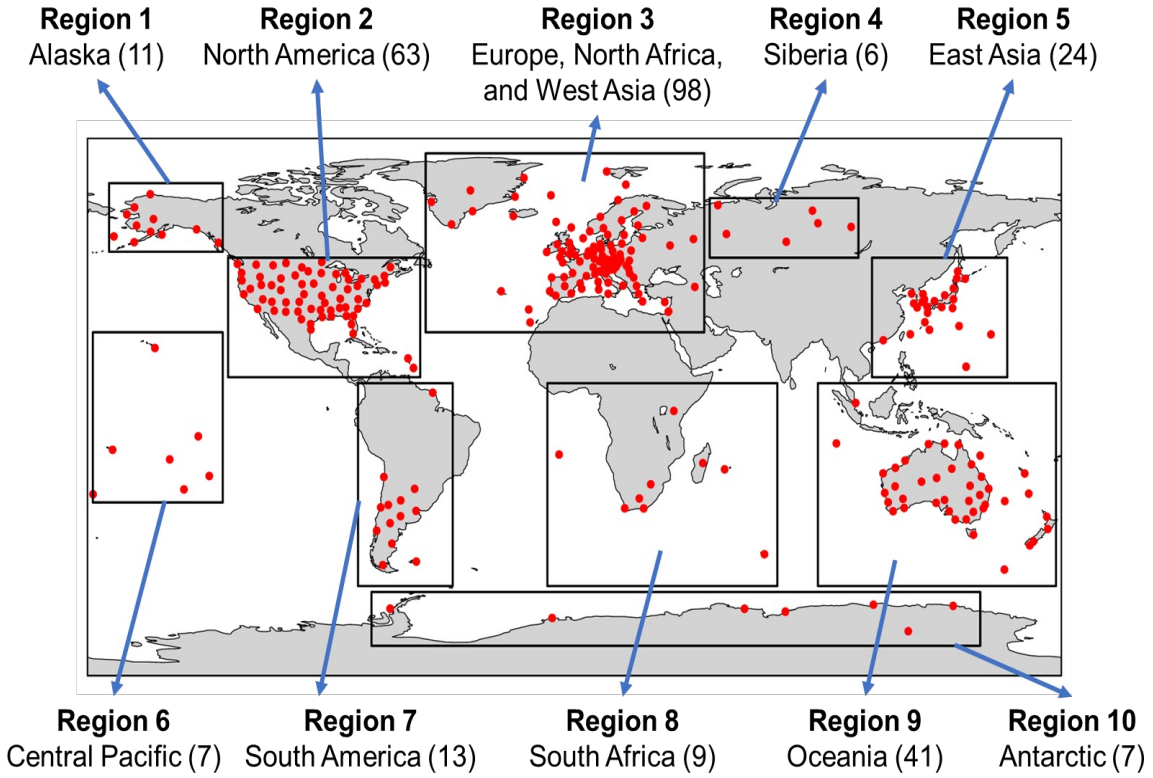

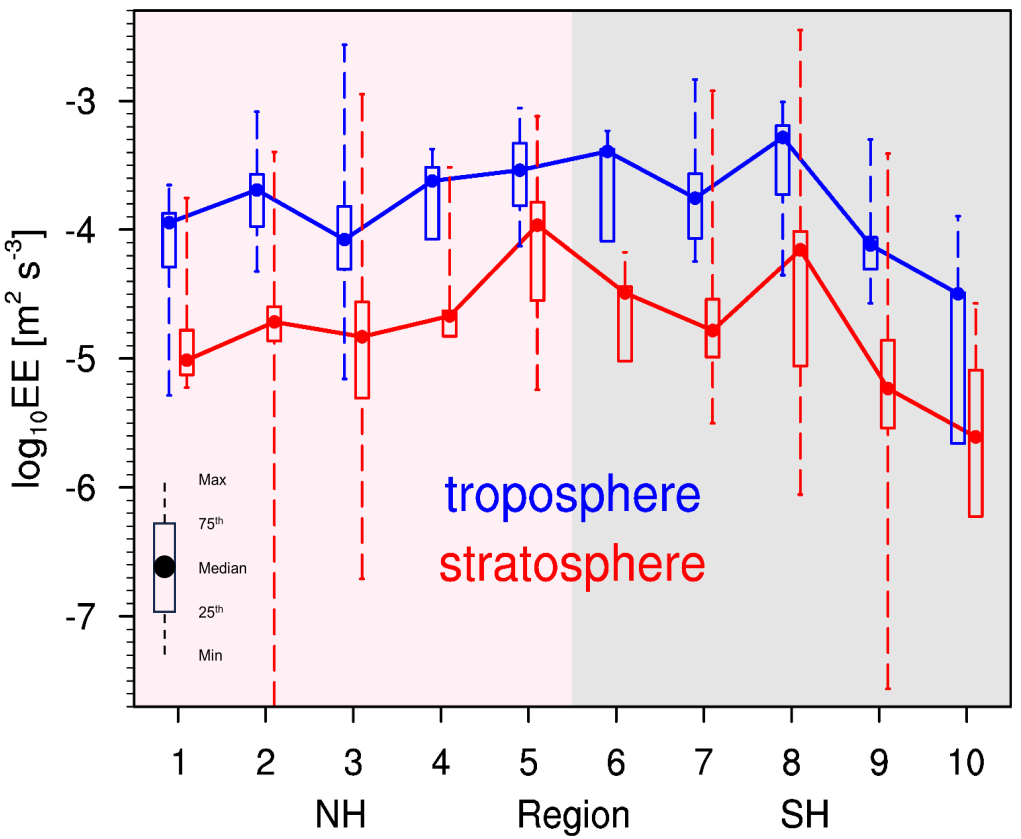

- $Log_{10}EE$ is generally larger in the troposphere than in the stratosphere, with significant variations in each sounding, especially in the stratosphere.
- **For median**: South Africa (R8) in SH and East Asia (R5) in NH are the largest in both the troposphere and stratosphere. Antarctic (R10) is the smallest in the troposphere and stratosphere.

  For maximum: Europe (R3) in NH and South America (R7) in SH is the largest in the troposphere, while South Africa is the largest in the SH stratosphere
- As numbers of profiles used for the analysis are very different from each region, further analyses are required.

Some Issues and On-going Research

- **Reliability of HVRRD-EDR can be examined by comparing with flight-EDR** (e.g., Ko et al. 2023), although **fundamental differences exist between the two data sets**, which are related to some limitations in each method.
  - Turbulence estimated using the Thorpe method and HVRRD is exclusively from convective instability, and **Kelvin-Helmholtz instability (KHI) under stable condition cannot be considered**. Improvement/modification of the Thorpe method is underway.
  - **Aircraft measurements may have a limitation accounting for the response to fluctuations at smaller scales than the aircraft size**. Large portion of the Thorpe scale (L_T) at main flight altitudes of commercial airlines is less than the size of flights.
- **The global HVRRD-EDR can be used for validation and improvement of global aviation turbulence forecasting systems** (e.g., GTG in USA and G-KGT in Korea), as supplementary to the flight-EDR of which data are provided only along the flight routes.
  - **Most of the turbulence forecasting systems include CAT and MWT diagnostics without considering near-cloud turbulence (NCT) diagnostics**, except for some recent efforts to include NCT diagnostics based on the convective GWD parameterization, representing turbulence by breaking of convective GWs above convection. (e.g., Kim et al., 2019; Kim et al., 2023).

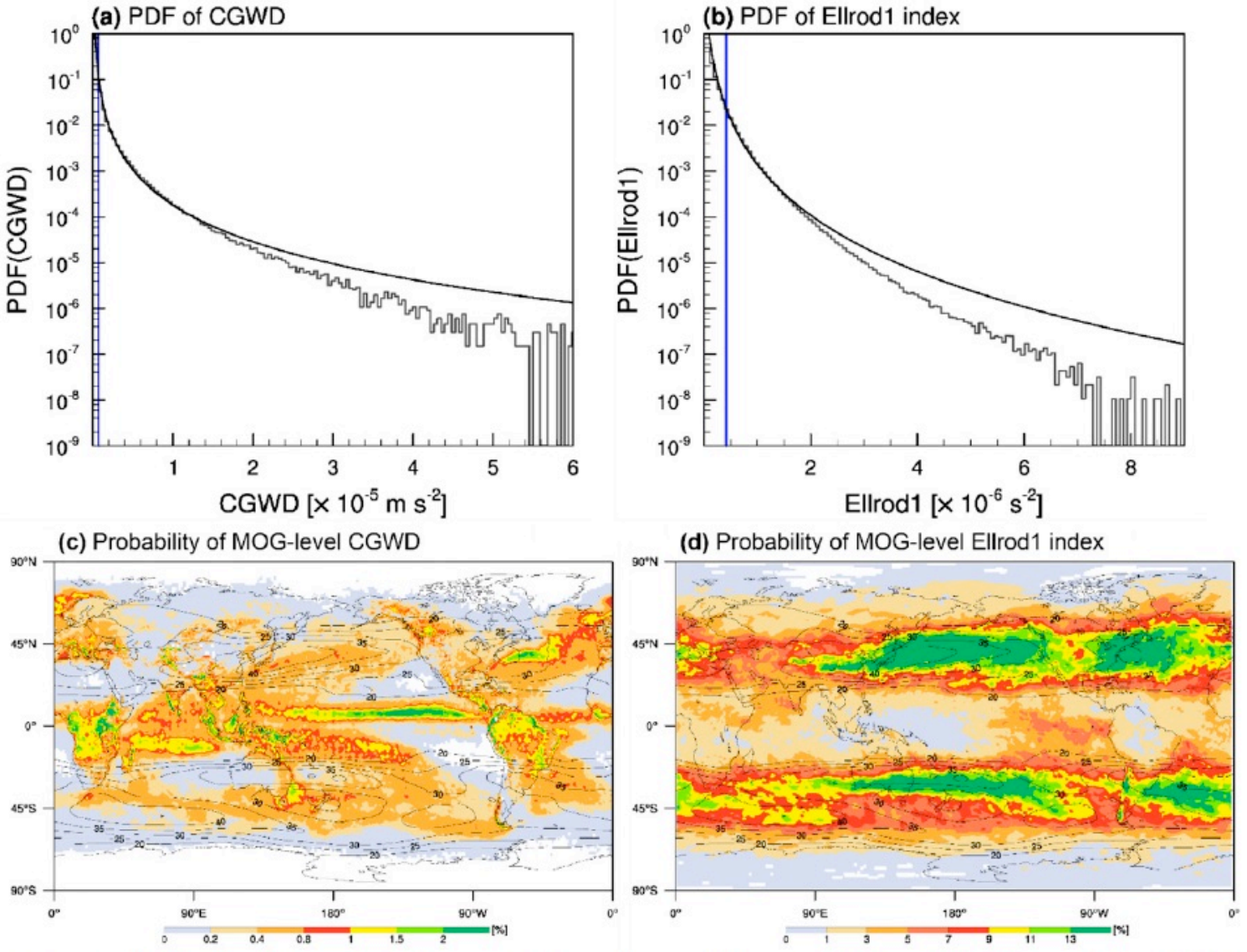

FIG. 18. (a),(b) The PDFs (histogram) and lognormal PDFs (continuous black line) of CGWD and Ellrod1 between 200 and 250 hPa calculated from December 2009 to November 2010 and (c),(d) the horizontal distributions of the probabilities of the MOG-intensity CGWD and Ellrod1 indices averaged from December 2009 through November 2010 between 200 and 250 hPa. The 95th percentile of CGWD and Ellrod1 is indicated by the blue line in (a) and (b). The superimposed mean wind (contour) between 200 and 250 hPa is shown in (c) and (d).

Development of Near-Cloud Turbulence (NCT) diagnostics based on a convective gravity-wave drag parameterization

S.-H. Kim, Chun, Sharman, Trier (2019, JAMC)

Dec. 2009-Nov. 2010 (1 yr) averaged over 200-250 hPa

Occurrence frequencies of MOG-level aviation turbulence under climate change scenario

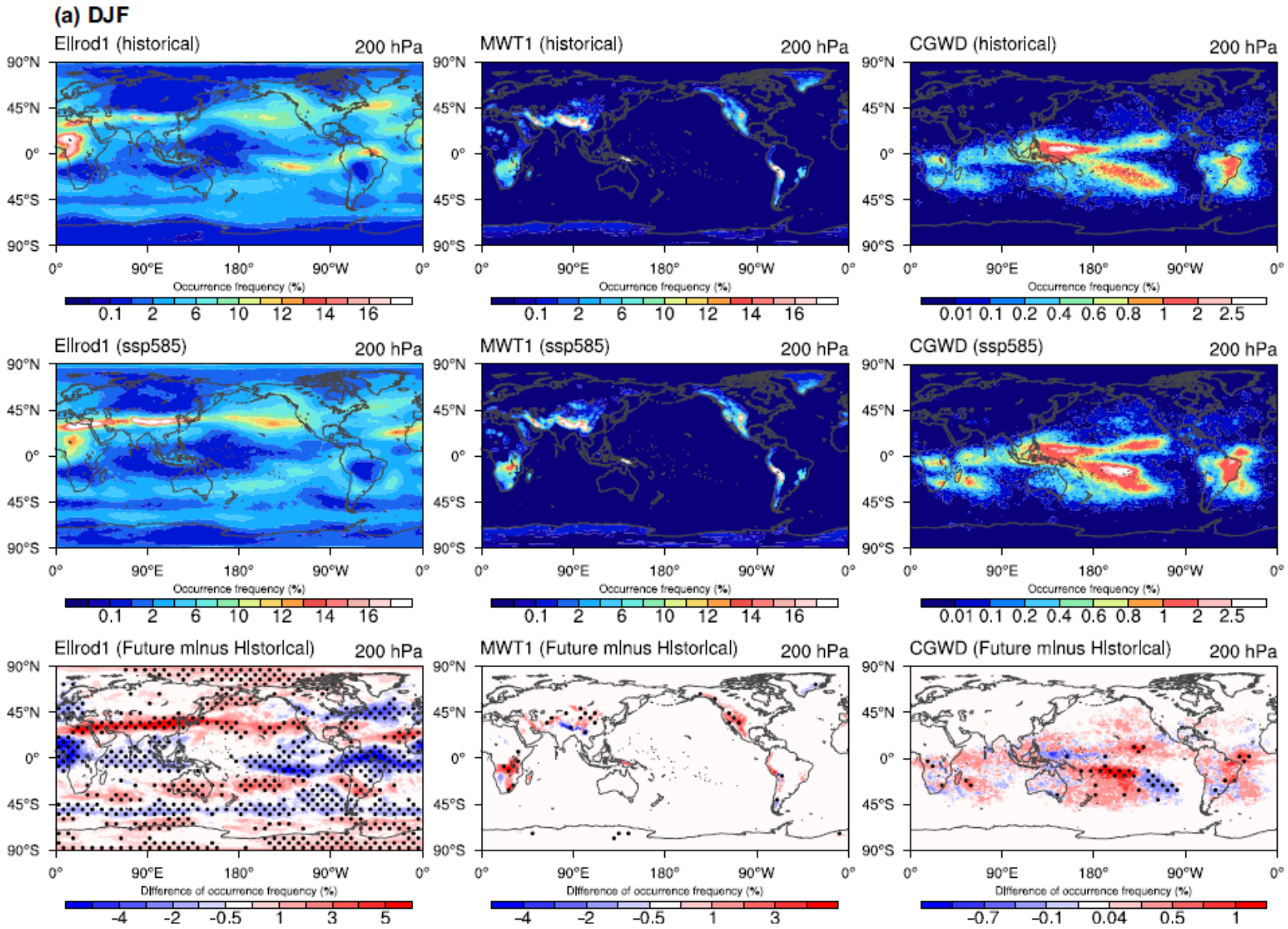

Impacts of climate change on the CAT, MWT, and NCT

S.-H. Kim, J.-H. Kim, Chun, Sharman (2023, npj climatsci)

Norwegian Earth System Model (NorESM2-MM)
- 1.25 x 0.94 (lon. x lat.)
- daily mean
- Historical: 1970-2014
- SSP5-8.5: 2056-2100

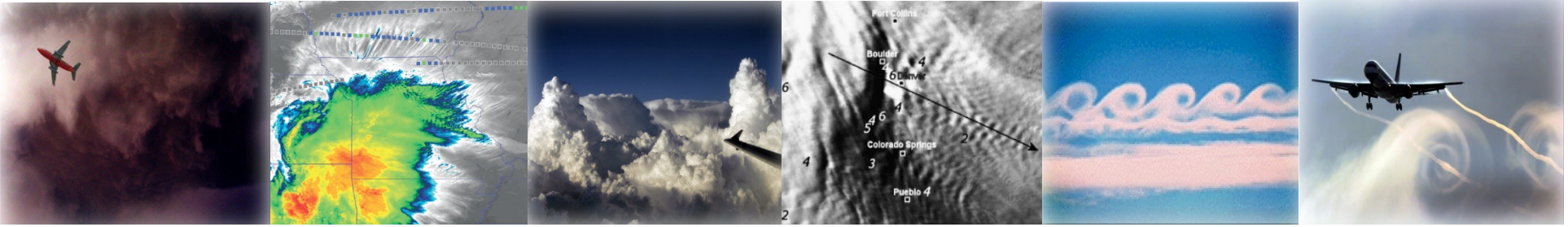

YONSEI UNIVERSITY

Thank you for your attention!

chunhy@yonsei.ac.kr